# Phenylalanine in the Pore of the *Erwinia* Ligand-Gated Ion Channel Modulates Picrotoxinin Potency but Not Receptor Function

Andrew J. Thompson, Mona Alqazzaz, Kerry L. Price, David A. Weston, and Sarah C. R. Lummis*

Department of Biochemistry, University of Cambridge, Cambridge CB2 1QW, U.K.

**ABSTRACT:** The *Erwinia* ligand-gated ion channel (ELIC) is a bacterial homologue of eukaryotic Cys-loop ligand-gated ion channels. This protein has the potential to be a useful model for Cys-loop receptors but is unusual in that it has an aromatic residue (Phe) facing into the pore, leading to some predictions that this protein is incapable of ion flux. Subsequent studies have shown this is not the case, so here we probe the role of this residue by examining the function of the ELIC in cases in which the Phe has been substituted with a range of alternative amino acids, expressed in *Xenopus* oocytes and functionally examined. Most of the mutations have little effect on the GABA $EC_{50}$, but the potency of the weak pore-blocking antagonist picrotoxinin at F16′A-, F16′D-, F16′S-, and F16′T-containing receptors was increased to levels comparable with those of Cys-loop receptors, suggesting that this antagonist can enter the pore only when residue 16′ is small. T6′S has no effect on picrotoxinin potency when expressed alone but abolishes the increased potency when combined with F16′S, indicating that the inhibitor binds at position 6′, as in Cys-loop receptors, if it can enter the pore. Overall, the data support the proposal that the ELIC pore is a good model for Cys-loop receptor pores if the role of F16′ is taken into consideration.

The *Erwinia* ligand-gated ion channel (ELIC) is a cation-selective GABA-gated ion channel originally identified in the enterobacterium *Erwinia chrysanthemii*. ELIC shares considerable structural homology with eukaryotic Cys-loop receptors, a class of neurotransmitter-gated ion channels that underpin fast synaptic transmission. One of the major problems in understanding the mechanisms of action of this family of channels is the paucity of high-resolution structures. An X-ray crystal structure of ELIC was determined in 2008, and the following year, the structure of the *Gloeobacter* ligand-gated ion channel or GLIC, from the bacterium *Gloeobacter violaceous*, was determined.[1−3] These bacterial receptors were found to share many structural features with Cys-loop receptors, although they do not possess an N-terminal α-helix, an intracellular domain, or the disulfide-bonded loop that gives the eukaryotic family its name. GLIC is activated by protons and ELIC by a range of small amine molecules, including GABA.[4,5] The potency of GABA at ELIC is low compared to those of its eukaryotic counterparts, but work on bacterial receptors in other systems[6,7] suggests that even if the potencies are not in the same range, their mechanisms of action at homologous proteins are similar, making ELIC an attractive model system for understanding the molecular mechanisms of Cys-loop receptors.

ELIC shows a low level of sequence identity with Cys-loop receptors overall, but many key features are conserved. The functional receptor is pentameric, with a large extracellular domain (ECD) that contains the ligand binding site and a transmembrane domain (TMD) consisting of four α-helices from each subunit (termed M1−M4). The M2 α-helix from each subunit lines the pore, and this region in particular is highly homologous in sequence (>60%) to Cys-loop receptors. It is, however, unusual in that it contains a large aromatic Phe residue that points into the pore lumen (Figure 1). This was proposed as
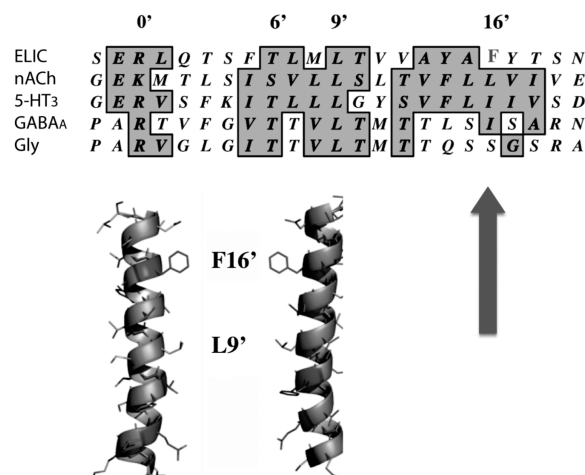


**Figure 1.** Alignment of M2 channel-lining residues for ELIC with eukaryotic Cys-loop receptors and a cartoon showing two of the five pore-forming transmembrane α-helices, highlighting the location of F16′ and L9′. As is common for these receptors, a prime notation is used to facilitate comparison between different subunits, with 0′ being the conserved charged residue at the start of M2. Accession numbers are P0C7B7 for ELIC, P46098 for 5-HT₃A, P02708 for nAChα1, P23415 for Gly α1, and P14867 for GABAₐ α1.

a reason that ELIC was not functional in early studies that sought to identify an activating ligand, a hypothesis supported by studies of molecular dynamics and Brownian dynamics.[8] Subsequent studies have shown that ELIC is readily opened by a range of

amine molecules,[4,5] and even when mutations are introduced to prevent desensitization, the structure of the pore is such that the Phe is present in the lumen.[9] As the pore has been used as a model for Cys-loop receptors, the aim of this study was to probe the role of this Phe residue, to determine if the ELIC channel is indeed representative of Cys-loop receptor pores.

## ■ MATERIALS AND METHODS

**Materials.** Picrotoxinin (PXN) was kindly provided by R. Duke (University of Sydney, Sydney, Australia) after separation and purification by recrystallization following short column vacuum chromatography from picrotoxin purchased from Sigma-Aldrich Australia. All other regents were from Sigma-Aldrich and of the highest grade that could be obtained.

**Cell Culture and Oocyte Maintenance.** *Xenopus laevis* oocyte-positive females were purchased from NASCO (Fort Atkinson, WI) and maintained according to standard methods. Harvested stage V and VI *Xenopus* oocytes were washed in four changes of $Ca^{2+}$-free ND96 [96 mM NaCl, 2 mM KCl, 1 mM $MgCl_2$, and 5 mM HEPES (pH 7.5)], defolliculated in 1.5 mg mL$^{-1}$ collagenase type 1A for approximately 2 h, washed again in four changes of ND96, and stored in ND96 at 16 °C containing 2.5 mM sodium pyruvate, 50 mM gentamycin, and 0.7 mM theophylline.

**Receptor Expression.** ELIC (GenBank accession number ADN00343.1) was kindly provided by C. Ulens. For expression in *Xenopus* oocytes, it was cloned into pGEMHE with the signal sequence of the human $\alpha$7 nACh receptor. Site-directed mutagenesis was performed with the QuikChange mutagenesis kit (Stratagene, La Jolla, CA). cRNA was transcribed *in vitro* from the linearized pGEMHE cDNA template using the mMessage mMachine T7 transcription kit (Ambion, Austin, TX). Stage V and VI oocytes were injected with 20 ng of cRNA, and currents were recorded 1−3 days postinjection.

**Electrophysiology.** Using two-electrode voltage clamp, *Xenopus* oocytes were clamped at −60 mV using an OC-725 amplifier (Warner Instruments, Hamden, CT), Digidata 1322A, and the Strathclyde Electrophysiology Software Package (Department of Physiology and Pharmacology, University of Strathclyde, Glasgow, U.K.). Currents were recorded at 5 kHz and filtered at a frequency of 1 kHz. Microelectrodes were fabricated from borosilicate glass (GC120TF-10, Harvard Apparatus, Edenbridge, Kent, U.K.) using a one-stage horizontal pull (P-87, Sutter Instrument Co., Novato, CA) and filled with 3 M KCl. Pipette resistances ranged from 1.0 to 2.0 MΩ. Oocytes were perfused with ND96 at a constant rate of 12 mL min$^{-1}$ with complete solution exchange within 5 s. Drug application was accomplished via a simple gravity-fed system calibrated to run at the same rate. Inhibition by test compounds was measured at the GABA $EC_{50}$ for each mutant.

Analysis and curve fitting were performed using Prism version 4.03 (GraphPad Software, San Diego, CA). Concentration−response data for each oocyte were normalized to the maximal current for that oocyte and the mean ± standard error of the mean (SEM) for a series of oocytes pooled and plotted against agonist or antagonist concentration and iteratively fit to the four-parameter logistic equation. Statistical analysis was performed using a Student's *t* test.

**Docking.** The three-dimensional structure of PXN was extracted from the Cambridge Structural Database (reference code PXN = CIBCUL10), and the protonated form was constructed using Chem3D Ultra 7.0 (CambridgeSoft, PerkinElmer, Waltham, MA) and energy-minimized using the MM2 force field. Docking

was as described previously[10] using an ELIC crystal structure (entry 2VL0) downloaded from the RCSB Protein Data Bank. Docking of PXN into ELIC was conducted using GOLD 3.0 (The Cambridge Crystallographic Data Centre, Cambridge, U.K.). The binding site was constrained as a docking sphere with a 20 Å radius surrounding either the $C_\alpha$ atom of residue 6′ or 16′ in chains A and C. Ten genetic algorithm runs were performed on each docking exercise using default parameters. The structures were visualized using PyMOL version 1.3 and ViewerLite version 5.0.

## ■ RESULTS

**Activation of ELIC by GABA.** ELIC has been previously shown to be activated by a range of small molecules containing an amine group, including cysteamine and GABA.[4,5] Here we used GABA, and its application produced large, concentration-dependent, reversible inward currents. Plotting peak current amplitude against a range of GABA concentrations yielded an $EC_{50}$ of 1.6 mM ($pEC_{50} = 2.78 \pm 0.04$; $n = 7$) and a Hill slope of $2.5 \pm 0.7$, similar to the values found in other studies.[4,5]

**Mutant Receptors.** To explore the role of phenylalanine in the pore of ELIC we substituted this residue with a selection of other amino acids covering a range of sizes and hydrophobicities, and we also introduced negatively charged residues as molecular dynamic simulation data have suggested that this will favor the open channel.[8] We observed some increases in $EC_{50}$ compared to those of wild-type receptors when we substituted Phe16′ with Glu, Leu, and Thr, but there were no significant changes to $EC_{50}$ with Ala, Asp, Gln, Trp, or Tyr (Table 1). These data show

**Table 1. Parameters Derived from GABA Concentration−Response Curves of Wild-Type and Mutant ELIC**

|  | GABA $EC_{50}$ | | | |
|---|---|---|---|---|
|  | $pEC_{50}$ | $EC_{50}$ (mM) | $nH$ | $n$ |
| wild type | $2.78 \pm 0.04$ | 1.6 | $2.5 \pm 0.7$ | 7 |
| Q2′A | NR$^a$ |  |  | 3 |
| Q2′N | $2.74 \pm 0.02$ | 1.8 | $2.6 \pm 1.3$ | 3 |
| T6′A | $3.07 \pm 0.01$ | 0.8 | $2.1 \pm 0.1$ | 3 |
| T6′S | $2.75 \pm 0.02$ | 1.8 | $2.7 \pm 0.3$ | 3 |
| F16′A | $2.31 \pm 0.08$ | 4.9 | $3.0 \pm 0.5$ | 4 |
| F16′D | $2.68 \pm 0.10$ | 2.1 | $2.5 \pm 0.3$ | 5 |
| F16′E | $1.59 \pm 0.05^b$ | 26 | $1.3 \pm 0.2$ | 3 |
| F16′Q | $2.11 \pm 0.10$ | 7.1 | $2.3 \pm 0.6$ | 3 |
| F16′L | $1.29 \pm 0.03^b$ | 51 | $1.6 \pm 0.2$ | 5 |
| F16′S | $2.15 \pm 0.06^b$ | 7.1 | $2.5 \pm 0.6$ | 4 |
| F16′T | $1.94 \pm 0.04^b$ | 11 | $1.8 \pm 0.3$ | 3 |
| F16′W | $2.64 \pm 0.02$ | 2.3 | $3.6 \pm 0.5$ | 3 |
| F16′Y | $2.12 \pm 0.10$ | 7.5 | $2.1 \pm 0.3$ | 5 |
| F16′S/T6′S | $2.19 \pm 0.09$ | 6.4 | $2.2 \pm 0.7$ | 3 |

$^a$No response at 100 mM GABA. $^b$Significantly different from that of the wild type ($p < 0.05$).

many residues are tolerated at this location, and that no specific chemical properties (such as aromaticity or hydrophobicity) are required. The negatively charged amino acids Glu and Asp have different effects: Asp at this position yielded an $EC_{50}$ similar to those of wild-type receptors, while Glu caused a 16-fold increase in $EC_{50}$. As residue 16′ is some distance from the binding site, these data suggest that it may play some minor role in channel gating (as the term $EC_{50}$ includes contributions from both binding and gating), although we cannot rule out the fact that this

and some of the other mutations may cause a global structural change that affects the binding site. However, as many pore-lining substitutions in many Cys-loop receptors have not been reported to cause a global structural change, we consider this less likely. The largest change in $EC_{50}$ was for Leu, which is surprising as Leu is found at position 16′ in many nACh receptor subunits, but these data are consistent with the fact that the structure in this region differs from that of its eukaryotic relatives.

We also made mutations at the Q2′ and T6′ positions. Q2′N, T6′A and T6′S mutations caused no change to the GABA EC50 values. Q2′A receptors did not respond to application of 100 mM GABA suggesting that they were either non-functional or not expressed. F16′S in combination with T6′S (T6′S/F16′S) caused no significant increase in EC50.

**PXN Inhibition.** Wild-type ELIC was inhibited by PXN with an $IC_{50}$ of 72 $\mu$M, similar to previous findings.[10] This value is considerably lower than values reported for GLIC and other Cys-loop receptors where it is known to bind in the pore and suggests that PXN mediates its action in ELIC by binding elsewhere on the protein. Given the homology between the M2 regions of all these receptors, it is surprising that PXN cannot bind, and thus, we considered whether a PXN binding site could exist in the pore and whether PXN cannot access this site because of the narrow entrance resulting from the presence of a ring of Phe residues at position 16′. We therefore examined the potency of PXN over a range of mutant receptors where the size of the residue was varied. These data showed that substitution with residues smaller than Phe increased PXN potency (Table 2, 3

**Table 2. Picrotoxinin Potencies of Wild-Type and Mutant ELICs[a]**

| | $pIC_{50}$ | $IC_{50}$ ($\mu$M) | $nH$ | $n$ |
|---|---|---|---|---|
| wild type | $4.14 \pm 0.05$ | 72 | $1.3 \pm 0.3$ | 3 |
| Q2′N | $4.36 \pm 0.07$ | 44 | $1.6 \pm 0.3$ | 3 |
| T6′A | $4.02 \pm 0.05$ | 95 | $1.8 \pm 0.4$ | 3 |
| T6′S | $4.17 \pm 0.08$ | 68 | $1.3 \pm 0.3$ | 3 |
| F16′A | $4.78 \pm 0.08^b$ | 16 | $1.0 \pm 0.2$ | 5 |
| F16′D | $5.03 \pm 0.11^b$ | 9.4 | $1.0 \pm 0.2$ | 3 |
| F16′W | $4.28 \pm 0.08$ | 52 | $1.3 \pm 0.3$ | 4 |
| F16′S | $5.35 \pm 0.07^b$ | 4.5 | $1.3 \pm 0.3$ | 3 |
| F16′T | $5.14 \pm 0.07^b$ | 7.2 | $0.9 \pm 0.1$ | 3 |
| F16′E | $4.57 \pm 0.12$ | 26.9 | $0.6 \pm 0.1$ | 3 |

[a]Data are means $\pm$ SEM. [b]Significantly different from that of the wild type ($p < 0.05$).

**Table 3. Picrotoxinin and Proadifen Potencies Are Differentially Modified in Pore-Lining Mutant ELICs[a]**

| | PXN | | proadifen | |
|---|---|---|---|---|
| | $pIC_{50}$ | $IC_{50}$ ($\mu$M) | $pIC_{50}$ | $IC_{50}$ ($\mu$M) |
| wild type | $4.14 \pm 0.05$ | 72 | $5.09 \pm 0.04$ | 8.1 |
| T6′S | $4.17 \pm 0.08$ | 68 | $5.59 \pm 0.12$ | 2.9 |
| F16′S | $5.35 \pm 0.07^b$ | 4.5 | $5.29 \pm 0.04$ | 5.1 |
| T6′S/F16′S | $4.36 \pm 0.05$ | 44 | $6.03 \pm 0.18$ | 0.9 |

[a]Data are means $\pm$ SEM ($n = 3-6$). [b]Significantly different from that of the wild type ($p < 0.05$).

and Figure 2), resulting in $IC_{50}$ values more similar to those observed with GLIC and Cys-loop receptors. A plot of $pIC_{50}$ versus side chain size (Figure 4) shows a distinct relationship ($R^2 = 0.7$), supporting our hypothesis, although there are some anomalies, such as the relatively high $IC_{50}$ for F16′A; we
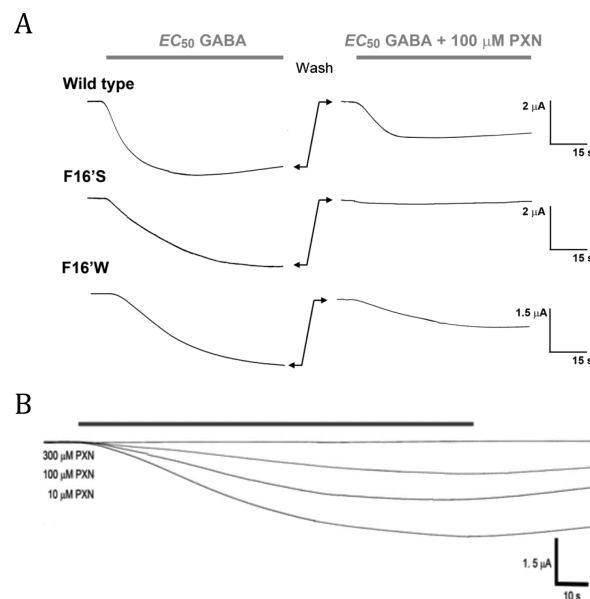


**Figure 2.** Example traces of PXN inhibition of wild-type and mutant ELIC. (A) Co-application of GABA $EC_{50}$ with 100 $\mu$M PXN inhibits $\sim$50% of the wild-type and F16′W responses but completely abolishes the F16′S response. (B) Increasing concentrations of PXN sequentially diminish the GABA-elicited response (here 0, 10, 100, and 300 $\mu$M PXN with 0.8 mM GABA). Data such as these were used to create the inhibition curves shown in Figure 3.
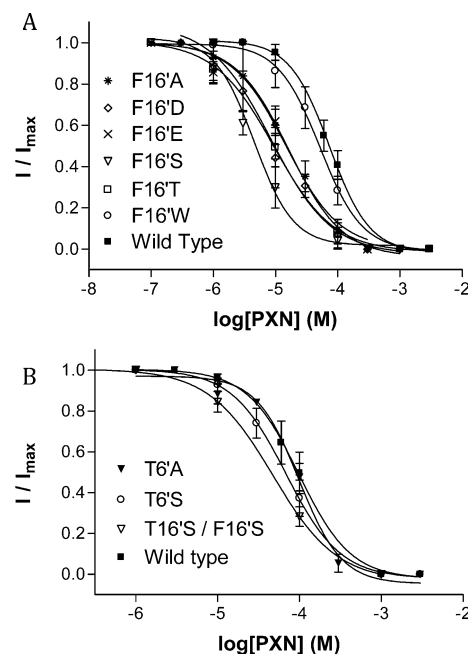


**Figure 3.** PXN inhibition of wild-type and mutant ELIC. (A) Inhibition curves of wild-type and F16′ mutant ELIC responses. (B) Inhibition curves of wild-type and T6′ mutant ELIC responses. Data are means $\pm$ SEM ($n = 3-6$). Parameters obtained from these curves are listed in Tables 2 and 3.

speculate that this may be due to extra flexibility in this region caused by insertion of a small residue.

Combining the F16′S and T6′S mutations ablated the increase in PXN potency, indicating that even when PXN can access the pore, it has specific binding requirements which involve T6′ (Table 3).
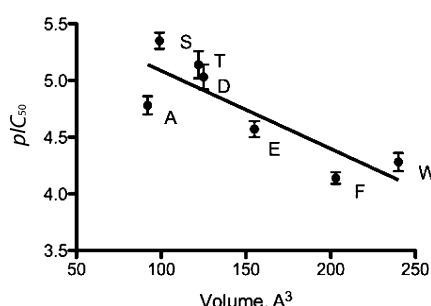
**Figure 4.** pIC$_{50}$ vs side chain volume. Volumes are calculated from the surface area of the side chain.[26]



**Figure 6.** Example docked pose for PXN in the ELIC channel. PXN is located close to the Thr residues at position 6′, where it is stabilized by hydrogen bonds. The channel is seen from the top looking down toward the cell interior.

**Proadifen Inhibition.** To further confirm our hypothesis that high-affinity inhibition by PXN depends on it being able to access its binding site deep in the pore and was not due to changes in other properties caused by the mutations, we examined inhibition by another compound that does not act via a pore binding site. Proadifen was one of the most potent inhibitors we previously identified in ELIC with an IC$_{50}$ of 8 $\mu$M.[10] Unlike that of PXN, the potency of this compound did not change when we examined its effects in F16′S, T6′S and F16′S/T6′S mutant ELIC (Table 3), consistent with a site of action that is not in the ion-permeable pore. These data also support our assumption that there has been no global change in the structure of ELIC caused by the pore-lining mutations.

**Docking Data.** The binding orientation and location of PXN have been studied in a number of Cys-loop receptors using ligand docking (with homology models where structures are not known) and have shown that it is deep in the pore, close to positions −2′, 2′, and/or 6′. These data allow potential molecular interactions to be identified and tested. As the structure of ELIC is known, it provides the opportunity for similar *in silico* studies here, although some caution must be applied, as the structure most likely is in the closed state. We docked PXN into the ELIC pore and identified possible binding poses in two regions: above F16′ and close to position 6′. Examination of multiple poses for those molecules bound close to F16′ revealed that the locations of PXN were broadly similar but that there were some variations in orientations; a similar finding was observed for PXN bound close to position 6′ (see Figure 5). One orientation of PXN close
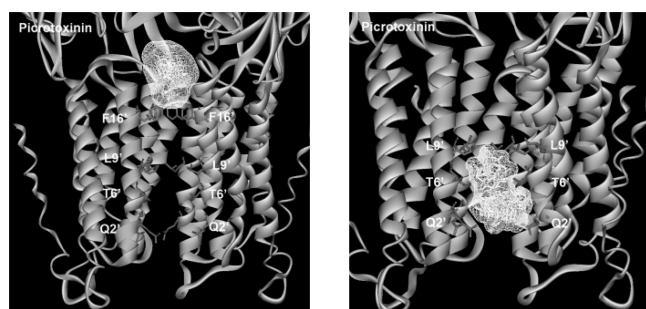


**Figure 5.** Overlay of 10 docked poses for PXN in the ELIC pore. The channel is seen from the side, and the ligands are located above F16′ (left) or close to the residues at position 6′ (right).

to position 6′ is shown in Figure 6, where it can be seen to be stabilized by several hydrogen bonds with the Thr residues at position 6′, which is consistent with a high-affinity binding site at this location. These data therefore support our hypothesis that PXN could bind in the pore with high affinity at a location that
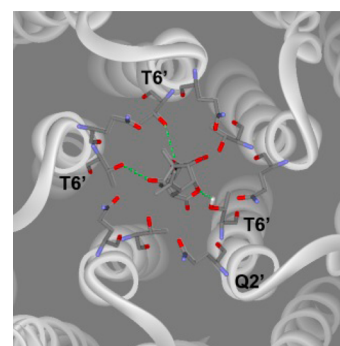
would be expected given its homology to Cys-loop receptor pores.

## ■ DISCUSSION

ELIC is a cationic GABA-gated bacterial ligand-gated ion channel that is functionally and structurally similar to vertebrate GABA-gated receptors.[10] ELIC has the advantage of a known high-resolution structure, making it a potentially useful system for understanding structure−function relationships in eukaryotes. However, the ELIC pore is unusual as it possesses a Phe residue at position 16′ that faces into the channel lumen (Figure 1); this might be expected to impede channel access. Here we show that this is the case for the channel blocking compound PXN, but increasing or decreasing the size of residue 16′ does not cause major changes to GABA-induced activation, indicating that the properties of the residue at this location do not significantly modify receptor function.

We have previously shown that many Cys-loop receptor pore blockers also block the pores of ELIC and GLIC but are generally less potent at ELIC.[10,11] Docking studies indicate that the 2′ and/or 6′ channel-lining residues are likely binding sites for many of these compounds in ELIC, and there are many mutagenesis studies in Cys-loop receptors that demonstrate the importance of these two residues (e.g., refs 12−15). Similarly, mutations of residues 2′ and 6′ in ELIC abolish inhibition by $\alpha$-endosufan, one of the most potent noncompetitive antagonists of this receptor, supporting a binding location close to these two residues. However, despite the similarity of pore-lining residues, PXN is more than 1 order of magnitude less potent in ELIC than in GLIC, where it has a potency similar to those of Cys-loop receptors.[10,11] The data presented here provide a solution to this apparent conundrum, as substitution of Phe16′ with a smaller residue such as Ser results in an IC$_{50}$ for PXN (4.5 $\mu$M) that is similar to that observed for GLIC (2.6 $\mu$M) and those observed for Cys-loop receptors.[16,17] Substitution with a larger residue, such as Trp, has no effect on the PXN IC$_{50}$. Our data therefore suggest that Phe at position 16′ sterically blocks the access of large pore binding antagonist molecules to the channel, while smaller residues do not. The fact that high concentrations of PXN block wild-type ELIC suggests that it has a low-affinity site of action elsewhere on the protein, as has been also suggested for GABA$_A$ receptors (e.g., ref 18).

Our data support our *in silico* studies that indicate the PXN pore binding site is close to position 6′: mutation of this residue has a significant effect on potency only when the residue is accompanied by an F16′S mutation, suggesting that PXN can

enter the pore and bind close to residue 6′ only when there is a small residue at position 16′. A site of action at position 6′ is consistent with the effects of mutating homologous residues in 5-HT₃, GABA, and glycine receptors; in these proteins, alterations to residue 6′ have significant effects on the sensitivity of PTX,[15,16,19] and these results are therefore similar to the results we obtained in our modified ELIC. It should be noted, however, that in GluCl picrotoxin may bind in a slightly different location, as the structural data reveal it is located further to the intracellular side of the pore, close to residue −2′.[20]

We also probed inhibition by the local anesthetic proadifen. This is not a classic Cys-loop channel blocker, although inhibitory effects have been reported.[21] The IC₅₀ values for proadifen did not change much with any of the pore-lining mutations. These data support the proposal that proadifen stabilizes the desensitized state of the receptor by acting at a site outside the channel pore, as has been proposed for nACh receptors,[21] and also supports our suggestion that the pore mutations do not globally change ELIC structure. Binding sites outside the pore have been identified using mutagenesis, photolabeling in Cys-loop receptors, and crystal structures of ELIC and GLIC bound with the general anesthetics bromoform, propofol, and desfluorane.[22−24]

Our data also reveal that F16′ can be substituted with residues that have quite distinct chemical properties without having major effects on EC₅₀ values, as previously shown for an F16′A mutant (<10-fold change in cysteamine EC₅₀), indicating that the residue at this location does not significantly affect receptor function. The largest changes we observed in EC₅₀ (32- and 16-fold) were for F16′L and F16′E, respectively. An increase with F16′L was unexpected as residue 16′ is Leu in many Cys-loop receptors. We speculate it may be less favorable in ELIC because of the adjacent Tyr: recent studies have shown an engineered ring of F16′ residues in the nACh receptor results in a novel refractory conformation; however, in combination with an engineered ring of Y17′ residues, there was a high open probability even in the absence of ligand.[25] Thus, the context of amino acids in the pore is critical in this region.

The increase observed for the F16′E alteration was less unexpected: charged residues are rarely found lining Cys-loop pores, where presumably they could inhibit ion flux (e.g., by repelling or binding to charged ions passing through the channel), or they may be thermodynamically unfavorable (e.g., similar charges may face each other). Nevertheless, a recent molecular dynamics study probing the possible effect of F16′E in ELIC concluded that such an alteration would have a favorable effect on the receptor: it suggested that the pore would be more hydrated, and the protein would have a more dynamic channel, exhibiting more movement of the pore-lining α-helices.[8] However, our observed increase in EC₅₀ suggests it is less favorable. We did not observe a similar increase with F16′D, suggesting that the longer side chain of Glu is responsible. Substitutions with Ser and Thr also caused small increases in EC₅₀, but all were <10-fold, indicating no major effect. Replacement with Trp had no effect, demonstrating that there is sufficient space at this location to accommodate a residue even larger than Phe.

In conclusion, we have demonstrated that the F16′ residue at the extracellular end of the ELIC pore does not play a major role in the function of the protein, as its replacement with a range of other amino acids has no major effect on GABA-activated currents. This residue may, however, prevent access of large, pore-blocking antagonists from reaching their binding sites lower

in the channel. Overall, our data can explain why channel blockers have lower potencies in ELIC than at either GLIC or Cys-loop receptors and show that using ELIC as a model for interactions with such compounds (for in silico and functional studies) is likely to be more accurate if their entry into the pore is permitted by substitutions of F16′.

## ■ AUTHOR INFORMATION

### Corresponding Author
*Department of Biochemistry, Tennis Court Road, Cambridge CB2 1QW, U.K. E-mail: sl120@cam.ac.uk. Telephone: (+44) 1223 765950. Fax: (+44)1223 333345.

### Notes
The authors declare no competing financial interest.

## ■ ABBREVIATIONS

nACh, nicotinic acetylcholine; AChBP, acetylcholine binding protein; GABA, γ-aminobutyric acid; ELIC, Erwinia ligand-gated ion channel; GLIC, Gloeobacter ligand-gated ion channel; PXN, picrotoxinin; ACh, acetylcholine; 5-HT, 5-hydroxytryptamine.

## ■ REFERENCES

(1) Bocquet, N., Nury, H., Baaden, M., Le Poupon, C., Changeux, J. P., Delarue, M., and Corringer, P. J. (2009) X-ray structure of a pentameric ligand-gated ion channel in an apparently open conformation. Nature 457, 111−114.
(2) Hilf, R. J., and Dutzler, R. (2009) Structure of a potentially open state of a proton-activated pentameric ligand-gated ion channel. Nature 457, 115−118.
(3) Hilf, R. J., and Dutzler, R. (2008) X-ray structure of a prokaryotic pentameric ligand-gated ion channel. Nature 452, 375−379.
(4) Spurny, R., Ramerstorfer, J., Price, K., Brams, M., Ernst, M., Nury, H., Verheij, M., Legrand, P., Bertrand, D., Bertrand, S., Dougherty, D. A., de Esch, I. J., Corringer, P. J., Sieghart, W., Lummis, S. C., and Ulens, C. (2012) Pentameric ligand-gated ion channel ELIC is activated by GABA and modulated by benzodiazepines. Proc. Natl. Acad. Sci. U.S.A. 109, E3028−E3034.
(5) Zimmermann, I., and Dutzler, R. (2011) Ligand Activation of the Prokaryotic Pentameric Ligand-Gated Ion Channel ELIC. PLoS Biol. 9, e1001101.
(6) Singh, S. K., Yamashita, A., and Gouaux, E. (2007) Antidepressant binding site in a bacterial homologue of neurotransmitter transporters. Nature 448, 952−956.
(7) Zhou, Z., Zhen, J., Karpowich, N. K., Goetz, R. M., Law, C. J., Reith, M. E., and Wang, D. N. (2007) LeuT-desipramine structure reveals how antidepressants block neurotransmitter reuptake. Science 317, 1390−1393.
(8) Cheng, X., Ivanov, I., Wang, H., Sine, S. M., and McCammon, J. A. (2009) Molecular-dynamics simulations of ELIC: A prokaryotic homologue of the nicotinic acetylcholine receptor. Biophys. J. 96, 4502−4513.
(9) Gonzalez-Gutierrez, G., Lukk, T., Agarwal, V., Papke, D., Nair, S. K., and Grosman, C. (2012) Mutations that stabilize the open state of the Erwinia chrisanthemi ligand-gated ion channel fail to change the conformation of the pore domain in crystals. Proc. Natl. Acad. Sci. U.S.A. 109, 6331−6336.
(10) Thompson, A. J., Alqazzaz, M., Ulens, C., and Lummis, S. C. (2012) The pharmacological profile of ELIC, a prokaryotic GABA-gated receptor. Neuropharmacology 63, 761−767.

(11) Alqazzaz, M., Thompson, A. J., Price, K. L., Breitinger, H. G., and Lummis, S. C. (2011) Cys-loop receptor channel blockers also block GLIC. *Biophys. J. 101*, 2912−2918.

(12) Hawthorne, R., and Lynch, J. W. (2005) A picrotoxin-specific conformational change in the glycine receptor M2-M3 loop. *J. Biol. Chem. 280*, 35836−35843.

(13) Sedelnikova, A., Erkkila, B. E., Harris, H., Zakharkin, S. O., and Weiss, D. S. (2006) Stoichiometry of a pore mutation that abolishes picrotoxin-mediated antagonism of the GABA$_A$ receptor. *J. Physiol. 577*, 569−577.

(14) Buhr, A., Wagner, C., Fuchs, K., Sieghart, W., and Sigel, E. (2001) Two novel residues in M2 of the $\gamma$-aminobutyric acid type A receptor affecting gating by GABA and picrotoxin affinity. *J. Biol. Chem. 276*, 7775−7781.

(15) Yang, Z., Cromer, B. A., Harvey, R. J., Parker, M. W., and Lynch, J. W. (2007) A proposed structural basis for picrotoxinin and picrotin binding in the glycine receptor pore. *J. Neurochem. 103*, 580−589.

(16) Das, P., and Dillon, G. H. (2005) Molecular determinants of picrotoxin inhibition of 5-hydroxytryptamine type 3 receptors. *J. Pharmacol. Exp. Ther. 314*, 320−328.

(17) Thompson, A. J., Duke, R. K., and Lummis, S. C. (2011) Binding Sites for Bilobalide, Diltiazem, Ginkgolide, and Picrotoxinin at the 5-HT$_3$ Receptor. *Mol. Pharmacol. 80*, 183−190.

(18) Carpenter, T. S., Lau, E. Y., and Lightstone, F. C. (2013) Identification of a possible secondary picrotoxin-binding site on the GABA$_A$ receptor. *Chem. Res. Toxicol. 26*, 1444−1454.

(19) Erkkila, B. E., Sedelnikova, A. V., and Weiss, D. S. (2008) Stoichiometric pore mutations of the GABA$_A$R reveal a pattern of hydrogen bonding with picrotoxin. *Biophys. J. 94*, 4299−4306.

(20) Hibbs, R. E., and Gouaux, E. (2011) Principles of activation and permeation in an anion-selective Cys-loop receptor. *Nature 474*, 54−60.

(21) Spitzmaul, G., Gumilar, F., Dilger, J. P., and Bouzat, C. (2009) The local anaesthetics proadifen and adiphenine inhibit nicotinic receptors by different molecular mechanisms. *Br. J. Pharmacol. 157*, 804−817.

(22) Jayakar, S. S., Dailey, W. P., Eckenhoff, R. G., and Cohen, J. B. (2013) Identification of propofol binding sites in a nicotinic acetylcholine receptor with a photoreactive propofol analog. *J. Biol. Chem. 288*, 6178−6189.

(23) Nury, H., Van Renterghem, C., Weng, Y., Tran, A., Baaden, M., Dufresne, V., Changeux, J. P., Sonner, J. M., Delarue, M., and Corringer, P. J. (2010) X-ray structures of general anaesthetics bound to a pentameric ligand-gated ion channel. *Nature 469*, 428−431.

(24) Spurny, R., Billen, B., Howard, R. J., Brams, M., Debaveye, S., Price, K. L., Weston, D. A., Strelkov, S. V., Tytgat, J., Bertrand, S., Bertrand, D., Lummis, S. C., and Ulens, C. (2013) Multisite Binding of a General Anesthetic to the Prokaryotic Pentameric *Erwinia chrysanthemi* Ligand-gated Ion Channel (ELIC). *J. Biol. Chem. 288*, 8355−8364.

(25) Gonzalez-Gutierrez, G., and Grosman, C. (2010) Bridging the gap between structural models of nicotinic receptor superfamily ion channels and their corresponding functional states. *J. Mol. Biol. 403*, 693−705.

(26) Richards, F. M. (1977) Areas, volumes, packing and protein structure. *Annu. Rev. Biophys. Bioeng. 6*, 151−176.